計測自動制御学会東北支部　第１９４回研究集会　(2001.6.1)

資料番号　１９４－１０

Stability and Chaotic Behavior of Farm Tractors

O Leroy O. GARCIANO, Ryo TORISU, Jun-ichi TAKEDA and Jun Yoshida

Department of Agricultural Engineering, Faculty of Agriculture, Iwate University
Ueda 3-18-8, Morioka 020-8550, Japan, Tel:(019)621-6267, Fax:(019) 621-6204
email: garciano@hotmail.com

[Keywords] Stability, chaotic vibrations, nonlinear tractor dynamics, correlation dimension, Lyapunov exponent, random vibration, quasi-periodic vibration

1. Introduction

The use of larger tractors and the higher working speeds to sustain or increase productivity has been the trend due to the changing situation of Japanese farming systems. It has been reported that higher working speeds causes the deterioration of the tractor dynamics[1], and violent bouncing phenomena also arise when a small size tractor runs under certain road conditions, which may lead to fatal accidents[2),3)]. Therefore, the understanding of the dynamic behavior of the tractor is a fundamental concern.

Although much research has been done in these areas, almost all were conducted in the conventional approach using spectrum analysis except Sakai. Sakai first introduced the nonlinear dynamics standpoint to tractor dynamics, clarified the chaotic vibration and showed the safety limits. Especially, in the area of steering and handling, nonlinear behavior of the tractor plays an important role on the stability of the tractor system.

The objectives of this paper are to investigate the dynamic stability, and chaotic behavior of a farm tractor assumed as a rigid body on a wide range of forward speeds.

2. Methodology

2.1 Experimental set-up

The tractor used was a pneumatic-tired John Deere model 2850D of 65 kW rating equipped with front tires 13.6-24 and rear tires 16.9-34. The total mass was 3690 kg with 2280 kg on the rear axle. The center of gravity was located 0.884 m in the front of the rear axle center and 0.933 m above the ground. Tire inflation pressure was set at 0.20 MPa in the front and 0.15 MPa in the rear. The wheelbase of the tractor was 2.29 m.

The artificial test track composed of a series of angle irons of height 0.035 m was installed on a gravel farm road and the spacing (wavelength) between the angle irons was set at 0.5 m with a total length of 25 m.

Tractor vibration was measured by two strain gage type linear accelerometers installed on the tractor chassis. The accelerometers measured the vertical components of vibration and their locations are shown in Fig. 1. Each accelerometer was labeled as A, and B and their capacities were 2g and 1g respectively. The recording instruments included a 4-channel analog data recorder and strain amplifier installed on the rear right side fender of the tractor. The picked-up signal was processed with a low pass filter of 30 Hz.

Rear wheel centerline Front wheel centerline

(b) Side view (a) Top view

Fig 1 Location of center of gravity of tractor and accelerometer

2.2 The frequency response test

A frequency response test was conducted using an artificial test track as the source of excitation to the tractor. In the experiment, all wheels run on the test track. In each run, the tractor forward speed was kept constant, so that the excitation was periodic and continuous, and the forced oscillation was a steady state. The forcing frequency f_1 of the forced vibration is expressed as $f_1=v/l$, where v is the forward speed and l the wavelength. In the experiment, the forward speed is chosen as the controlled parameter and the speed was varied from 0.63~4.50 m/s increased at intervals of 0.10~0.20 m/s for a total of 24 experimental runs.

2.3 Chaos time series analysis

In the experimental time series analysis, only the front A accelerometer signal were discussed. The rear B signal has the same tendency with the front with a time lag of wb/v, where wb is the wheelbase and v is the forward speed. The amplitude of vibration of B is lower when compared to A.

The post transient phase was decided and the sampling time was varied in the range of 0.01~0.005 s. In the sampling time of 0.01s the speed range was from 0.63~1.51 m/s and the total number of data points was in the range of 900~1800. In the sampling time of 0.005s, the speed range was from 1.61~4.50 m/s and the total number of data points was in the range of 960~1700. In diagnosing the types of vibrations, qualitative changes of the dynamics of the tractor due to the change in the forward speed, was analysed by embedding the time series in a state space using the method of time delay. A Poincare section was made by stroboscopic sampling of the time series, which can be used to distinguish between various qualitative states of motion such as periodic, quasi-periodic, or chaos. Quantitative analysis, using the correlation dimension to identify the types of vibrations, and trend of the largest Lyapunov exponents for deterministic chaos were also made.

(1) Qualitative analysis of the tractor vibrations

Phase portrait and Poincare sections

The phase portrait provides a spatial snapshot of the evolving dynamics of a nonlinear system as an aid in the understanding of how parameter changes affect the systems behavior. It is particularly useful in visualizing the dynamics of the system as the forward speed is changed. In the making of the phase portrait, the current value of a time series is related to the preceding value of the same series using a fixed delay time or lag.

A Poincare section is a sequence of points in phase space generated by the penetration of a continuous evolution trajectory through a generalized surface or plane in the space[4]. It is constructed by stroboscopic sampling of the time series at a fixed-phase of the forcing function that is the artificial test track.

(2) Quantitative analysis of the tractor vibrations

Two widely used criteria on the quantitative analysis of the motion of a dynamical system, which will either be chaotic or regular are the Lyapunov exponents and the correlation dimension.

(a) Correlation dimension analysis

From the experimental time series data, computing the correlation dimension (D) is useful for distinguishing deterministic and stochastic motion. For the attractor reconstructed in the m-dimensional phase space by the method of time delay, the correlation integral $C^m(r)$ [5] is defined for large N by,

$$C^m(r) = \lim_{N\to\infty} \frac{1}{N^2} \sum_{\substack{i,j=0 \\ i\neq j}}^{N-1} H(r - |X_i - X_j|) \tag{1}$$

where, H is the Heaviside function, r the radius of an n-dimensional hypersphere centered on each sampled point on the attractor trajectory, X_i, (I=1,2,3,...N) and X_j are the other points on the attractor in the vicinity of X_i. The term $|X_i - X_j|$ is calculated as a Euclidean distance in an m-dimensional space. The correlation dimension D is computed as the slope (s) of each curve of log C^m (r) versus log r.

(b) The Lyapunov exponent

Lyapunov exponents are the average exponential rates of divergence or convergence of nearby orbits in phase space of a given continuous dynamical system in an m-dimensional phase space. Thus, the exponents are related to the expanding and contracting nature of different directions in phase space. A positive Lyapunov exponent is defined to be chaotic, a zero exponent would indicate a marginally stable orbit, and a negative exponent would indicate periodic motion[6].

(b) Frequency domain analysis

Nonlinear resonance curve can identify at what particular frequency (speed) the tractor exhibits violent vibration phenomenon. Such a curve is useful in determing the natural frequencies of the tractor.

3. Results and Discussion

3.1 Chaos time series analysis

(1) The attractor reconstruction using the method of delay time

In the analysis of the experimental time series obtained from dynamics of the tractor, the trajectory of the post transient phase was analyzed as it approaches to its attractor. An attractor is a set of points in phase space that the nonlinear system approaches eventually starting from a set of points known as the basin of attraction[7].

The method of reconstructing the attractor within an embedding space of some suitable dimension m is called the method of time delay. From the time series, the attractor is made using an appropriate value of delay time τ. Different delay time of T/2, T/6 and T/4 were used for this purpose. The attractor is first embedded in a two dimension. A more rigorous way to estimate the actual dimension of the attractor using quantitative methods is presented later.

An example of the reconstruction of the attractor is *shown* in *Fig. 2. Figure 2.1~2.4 shows the* phase portrait from the reconstructed time series data of speed 2.15 m/s with an embedding dimension m=2. In Fig. 2.1, using a delay time of T/2, the attractor coordinates are formed from very closed points, hence there is a strong positive correlation and the attractor aligns itself almost along the $\angle -45^\circ$ dashed line.

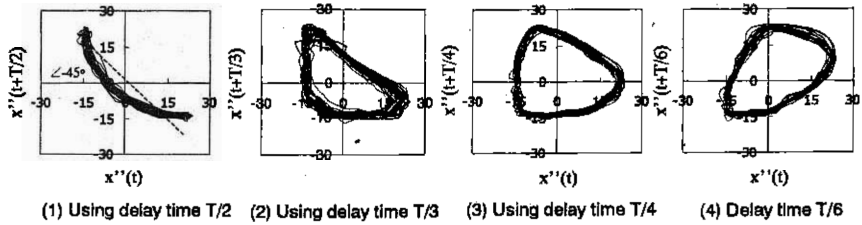

Figure 2. Attractor reconstruction of the time series data

However, from Fig. 2.2 and 2.4 shows three almost similar phase portraits using the delay time of T/3, T/4 and T/6 respectively. Here it is seen that as the time series points used for the attractor co-ordinates begin to separate and de-correlate, the attractor opens up in phase space. In this case, a visual inspection of the phase portrait of the resulting attractor which appears to give the minimum spread out attractor[8),9)] or as open as possible is the delay time T/4 which is used in the attractor reconstruction.

(2) Qualitative analysis

Phase portrait and Poincare section

The total number of experimental runs was 24. Therefore, there are 24 phase portraits and 24 Poincare sections. From these 24 pairs of graphs, six sample pairs were chosen as the representative.

Figure 3 shows the six sample pairs of phase portraits and Poincare section of the tractor vibration. The chosen speeds were 0.97 m/s, 1.51 m/s, 2.15 m/s, 2.88 m/s, 3.52 m/s and 4.32 m/s.

From Fig. 3.1, complex dynamics in the speed 0.97 m/s was observed due to the complex trajectory of the vibrations, and between 0.97 to 1.51 m/s (Fig. 3.1~3.2), a qualitative changed occurred due to the different shape of the trajectories, which can be seen, from these phase portraits.

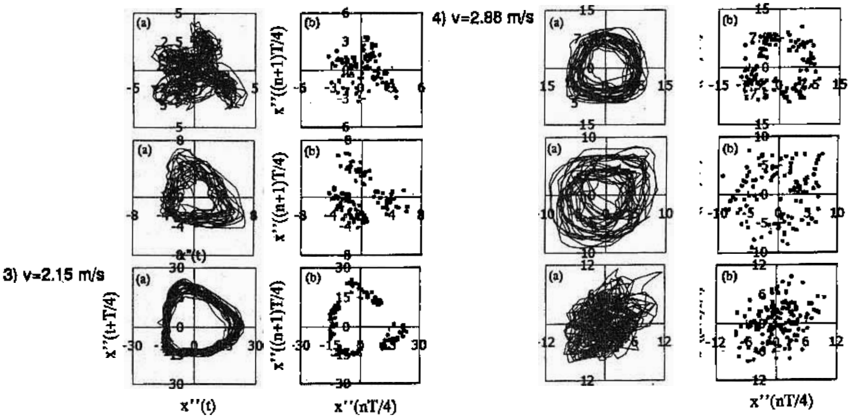

Figure 3 Representative samples of (a phase portrait and (b) Poincare sections at different forward speeds

From Fig. 3.2~3.4, the almost elliptical trajectory in the speeds of 2.15 m/s and 2.88 m/s were observed from the phase portrait. The Poincare section in Fig. 3.3(b) showed the points moving around in an approximate ellipse curve in the stroboscopic plane indicated a clear quasi-periodic vibration. Increasing the speed further from 3.52~4.32 m/s (Fig. 3.5~3.6) showed a qualitative changed from quasi-periodic to a complex vibration.

From Fig. 3, there are three types of qualitative dynamics. In the middle speed of 1.51 m/s to 2.15 m/s, is a quasi-periodic vibration. This is where the resonance frequencies of the tractor in the bounce and pitch mode occurred in the frequency range of 3.2 Hz 4.3~4.8 Hz[10] respectively. In the lower speed of 0.95 m/s, and in the higher speeds of 3.52 m/s and 4.32 m/s the types of vibrations could not be determined using the phase portrait and Poincare section.

(3) Classification of the types of vibrations from the qualitative changes of the tractor dynamics

Based from the difference or similarity of the phase portrait patterns, the types of vibrations were classified according to the low, middle, and high speeds. In the low speed, the range was from 0.63-1.42 m/s. In the middle speed, the range was from 1.51 m/s-3.08 m/s. In the high speed, the range was from 3.32-4.52 m/s.

In order to further explain the reason for the difference or similarity of the phase portrait, the time series and the frequency spectrum information were included. From Fig. 3, one speed each in the low, middle, and high speeds were chosen, and these are 0.97 m/s, 2.15 m/s, and 4.32 m/s respectively.

In the low speed of 0.97 m/s, a sample time series data is shown in Fig. 4. From this figure, the period of oscillation is 0.52 s. The frequency spectrum in Fig. 4b shows a fundamental forcing frequency f_1=2.0 Hz with other frequency influence, and dominant frequencies of 3.9 Hz and 5.9 Hz.

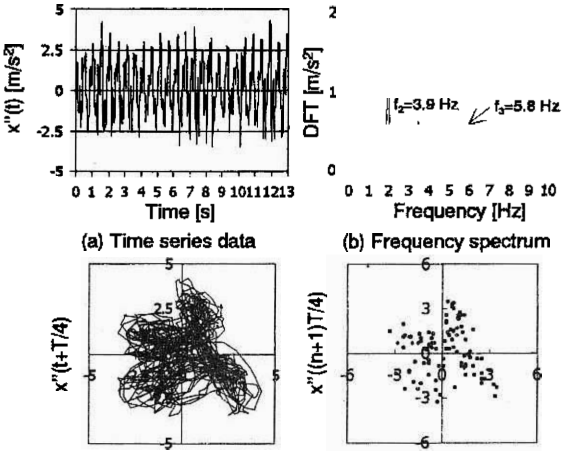

Figure 4. Complex vibration in the low speed of v=0.97 m/s

These other frequencies were probably due to the significant influence of the frequency spectrum of the gravel road where the angle irons were installed and tractor tire lugs. The resulting phase portrait and Poincare section in Fig. 4c and 4d respectively, showed a complex vibration, which were seen as scattered stroboscopic points in the Poincare' section. However, the type of vibration could not be determined using the phase portrait and Poincare section analysis.

In the high speed of 4.32 m/s, a sample time series data is shown in Fig. 5. From Fig. 5(a), the period of oscillation is 0.12 s. The frequency spectrum in Fig. 5b showed a fundamental frequency f_1=8.6 Hz and its subharmonic frequency $f_{1/2}$. Figure 5c and 5d shows the phase portrait and Poincare section respectively. The complex vibration is probably due to the influence of the subharmonic frequency $f_{1/2}$ that implied nonlinear vibration but the type of vibration could not be diagnosed clearly with the frequency information only.

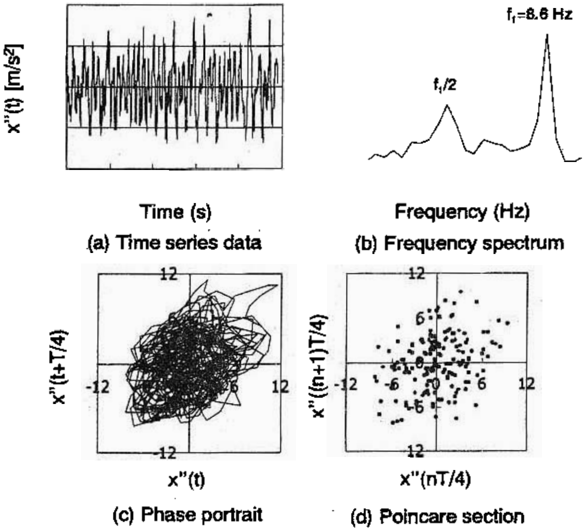

Figure 5 Complex vibration in the high speed of v=4.32 m/s

On the other hand, in the middle speed, a sample time series data of the vibration is shown in Fig. 6. The period of oscillation is 0.23 s. The frequency spectrum shown in Fig. 6b shows a dominant fundamental frequency f_1=4.3 Hz and with a superharmonic frequency component of $2f_1$ and the influence of f_2=4.6 Hz. The presence of the other frequency f_2 whose ratio f_2/f_1 is incommensurate indicated a quasi-periodic vibration. Thus, aside from the phase portrait and Poincare section information, the frequency spectrum was also helpful in classifying the types of vibrations.

On the other hand, in the middle speed, a sample time series data of the vibration is shown in Fig. 6. The period of oscillation is 0.23 s. The frequency spectrum shown in Fig. 6b shows a dominant fundamental frequency f_1=4.3 Hz and with a superharmonic frequency component of $2f_1$ and the influence of f_2=4.6 Hz. The presence of the other frequency f_2 whose ratio f_2/f_1 is incommensurate indicated a quasi-periodic vibration. Thus, aside from the phase portrait and Poincare section information, the frequency spectrum was also helpful in classifying the types of vibrations.

The above results show two classifications of vibrations. One group is classified as a complex vibration that occurred in the low and high-speed range, and the group was classified as quasi-periodic vibration that occurred in the middle speed range.

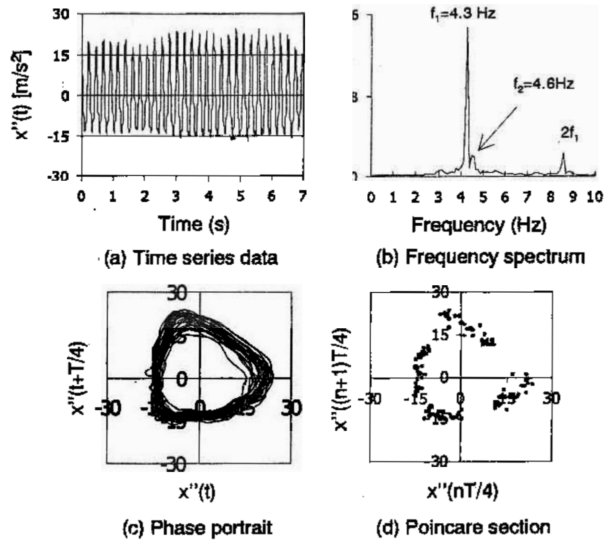

Figure 6 Quasi-periodic vibration in the middle speed of v=2.15 m/s

(4) Quantitative analysis

To diagnose the types of vibration in the low and high speeds that could not be determined using the qualitative methods, a quantitative analysis was conducted using the correlation dimension analysis and the Lyapunov exponent for the full range of the forward speed.

(a) Correlation dimension

The attractor reconstruction using the method of delay time was made using an embedding dimension (m) of two. To determine the actual m to contain the attractor of the experimental time series a correlation dimension D for the reconstructed attractor in embedding spaces of successively larger dimensions was conducted, using an algorithm that computes the D. The maximum m was set to 5.0. The radius (r) of the probing hyper sphere was from 1~10 units.

An example of a correlation dimension plot using a numerical algorithm is shown in Fig. 7 where the data was the time series at speed of v=2.14 m/s. The attractor was generated using N=1410 points. From Fig. 7a, with increasing m from 1~5, the slope (s) steadily diverges with increasing values of r due to the effect of noise. The noise is due to the nature of the input, the inherent characteristics of the system and noise contributed by the measuring instruments that were present in the output signal. Another factor is the effect of the computational noise[11] that arise due to round-off errors in the numerical computations that were made.

Since the test track was installed on a farm gravel road, random noise of the gravel road was present in the output signal. Dynamical system noise or system nonlinearity such as the spring stiffness and damping coefficients of the tractor tires are were also present in the output signal. The effect of the measurement noise and computational noise were not included in the analysis.

The limiting slope (Ls) was approximated to be equal to 1.19. Figure 7(b) is then plotted using the s versus log (r) where the curves converge at the limiting slope (encircled). Figure 7(c) is then made using the slope information with the increasing m, where the minimum saturation point was at m equal to 3.0, which is the appropriate embedding dimension of the attractor. Aside from the determination of the embedding dimension, a correlation dimension analysis was also made to determine the types of vibrations in the low and high speeds that could not be determined using qualitative analysis that was made in section (3).

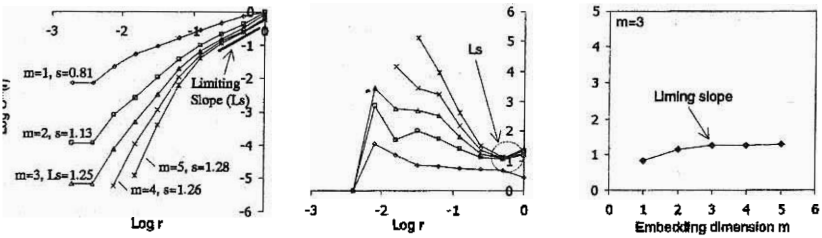

(a) The correlation integral Log C^m (r) versus Log r

(b) The correlation integral slope s=ΔLog C^m(r) ,/ΔLog r versus Log r

(c) Correlation dimension D vs. embedding dimension m

Fig. 7 (a) and (b) The correlation integral and (c) correlation dimension D vs. embedding dimension m at v=2.15 m/s

Figure 8 shows the correlation dimension D versus the embedding dimension m in the low, high and also in the middle speed. From Fig. 8(a), the steady increase of D as m was increased indicated that the attractor was not contained even in the fifth dimension. This suggests that the attractor is in the infinite dimension, which is a random vibration. From Fig. 8(b), D has a value of 3.61 that indicated chaotic vibration, and the attractor was contained in an m equal to 4. In Fig. 8(c), a D equal to 1.19 means quasi-periodic vibration and it reached saturation at m equal to 3.

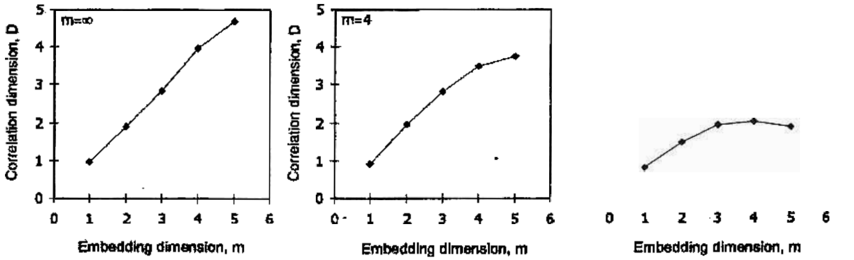

(a) Random vibration at v=0.97 m/s

(b) Chaos vibration at v=4.32 m/s

(c) Quasi-periodic vibration at v=1.50 m/s

Fig. 8 Correlation dimension (D) vs. embedding dimension (m)
(a) Low speed of v=0.97 m/s
(b) High speed of v=4.32 m/s
(c) Middle speed of v=1.50 m/s

(b) The Lyapunov exponent

Figure 9 shows the spectrum of the Lyapunov exponents (λ_i) versus the forward speeds with the equivalent forcing frequencies. Spurious Lyapunov exponents in the low speed range of 0.63~1.42 m/s was observed which is due to the significant influence of the gravel farm road in the experimental data, therefore, it was not included. Convergence of the Lyapunov exponents was attained by varying the attractor length scale and the constant propagation time (ref. 6). Starting from the middle speed range of 1.51 m/s, the type of vibration is quasi-periodic. The largest Lyapunov exponent which is a deterministic chaos[12] occurred at the frequency range of 7.0~9.0 Hz (speed range of 3.52~4.50 m/s).

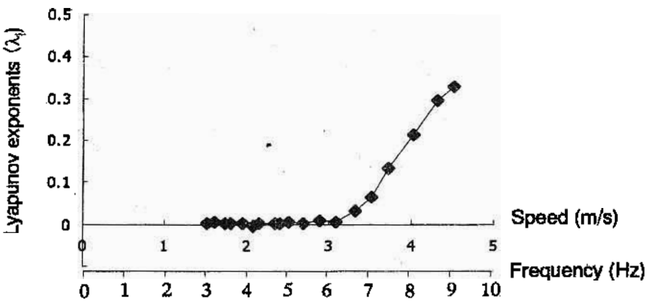

Fig. 9 Trend of the largest Lyapunov exponents
(Middle speed to high speed)

(5) Classifications of the types of vibrations according to the quantitative analysis of the tractor dynamics

Table 1 shows the classification of the types of vibrations using correlation dimension analysis and Lyapunov exponent estimates of the stability and chaotic behavior of the tractor. In the speed range of 0.63~1.42 m/s is a random vibration with an attractor dimension of more than 5. In the speed range of 1.50~3.08 m/s is a quasi-periodic vibration and marginal stability of the tractor behavior and the dimension of the attractor 3. In the speed range of 3.32~4.5 m/s is a chaotic vibration and the dimension of the attractor is 4.

Table 1. Classification of the types of vibrations according to the forward speed

Speed Classification	Speed range	Types of vibrations	Dimension of attractor
Low speed	0.63 ~ 1.42 m/s	Random vibrations	$m=\infty$
Middle speed	1.51~3.08 m/s	Quasi-periodic vibrations and marginal stability	m=3
High speed	3.32 ~ 4.52 m/s	Chaotic vibrations	m=4

3.2 Frequency domain analysis using the nonlinear resonance curve

Figure 10 shows the nonlinear resonance curve of the tractor vibrations. In the frequency of 3.2 Hz (speed of 1.6 m/s) is the bounce natural frequency, and in the frequency range of 4.2~4.8 Hz (2.1-2.4 m/s) is the pitch natural frequencies (ref. 10).

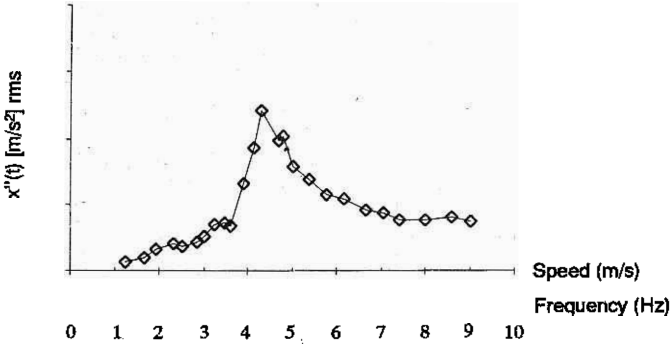

Fig. 10 Nonlinear resonance curve of the front A of the tractor chassis

4. Conclusions

The stability and chaotic behavior of a farm tractor assumed to be a rigid body was investigated from the standpoint of nonlinear tractor dynamics. In the experimental investigation, a frequency response test was conducted, and the analysis was carried out in the time domain and frequency domain analysis. In the time domain analysis, qualitative changes of the dynamic behavior of the tractor were analyzed using the phase portrait and Poincare section that identified the quasi-periodic vibrations in the middle speed range of 1.51 to 3.08 m/s. Quantitative analysis using the correlation dimension identified the random vibration in the low speed range of 0.63 to 1.42 m/s, and largest Lyapunov exponents analysis identified the deterministic chaotic vibrations in the high-speed range of 3.32~4.52 m/s. The tractor vibration resonance occurred in the middle speed range. The following conclusions can be drawn from the results obtained:

1. The effect of the gravel farm road produced random vibration that is significant in the low speed range that resulted to spurious Lyapunov exponent estimates.
2. Marginal stability of the tractor occurred in the middle speed range, which is a quasi-periodic vibration where the nonlinear resonance of the tractor occurred.
4. The subharmonic frequency $f_{1/2}$ that occurred at the higher speeds indicated chaotic vibrations of the tractor
5. Nonlinear tractor dynamics route to chaos was quasi-periodic from the middle speed range to chaos in the high-speed range.

References

1 Crolla, D. A., Horton, D. N.: Factors Affecting the Dynamic Behavior of Higher Speed Agricultural Vehicles, J. agric. Engng. Res., 30, 277-288,1984.
2 Sakai, K.: Experimental Analysis of Nonlinear Dynamics and Chaos in Bouncing Tractor, J. Japanese Soc. of Agricultural Machinery, 62(4), 63-70, 2000
3 Sakai, K.: Theoretical Analysis of Nonlinear Dynamics and Chaos in Bouncing Tractor, J. Japanese Soc. of Agricultural Machinery, 61(6), 65-71, 1999
4 Moon, F. C.: Chaotic and Fractal Dynamics: An Introduction for Applied Scientists and Engineers, John Wiley & Sons, Inc. p. 31, 1992
5 Sakai, K. Nonlinear Dynamics and Chaos in Agricultural Systems – for Agricultural Engineers, Analysts and Scientists-, Elsevire Science, pp. 3~4, 2002 (To be printed)
6 Wolf, Alan, Swift, J.B., Swinney, H.L., Vastanao, J.A.: Determining Lyapunov Exponents from a Time Series, Physica 16D, 285-317,1985.
7 Heath, Richard. A.: Nonlinear Dynamics: Techniques and Applications in Psychology, LEA Publishers, p. 165, 2000.

8 Addison, P.S.: Fractals and Chaos An Illustrated Course, Institute of Physics Publishing, pp. 164-167, 1997
9 Strogartz, S. H.: Nonlinear Dynamics and Chaos: With Applications to Physics, Biology, Chemistry and Engineering, Perseus Books, p. 441,1994.
10 Garciano, L., R. Torisu, J. Takeda, J. Yoshida: Resonance Identification and Mode Shape Analysis of Tractor Vibrations. J. Japanese Soc. Agricultural Machinery, 2001 (under review)
11 Albano, A.M., J. Muench, C. Schwartz: Singular-value decomposition and the Grassberger-Procaccia algorithm, Physical Review A 38(6), 3017-3026, 1988
12 Sakai, K.: Bifurcation Structure of Vibrations in an Agricultural Tractor-Vibrating Subsoiler System, Int'l. J. of Bifurcation and Chaos, 9(10), 1999.